

# Shortcuts to adiabatic state transfer in time-modulated two-level non-Hermitian systems

Qi-Cheng Wu<sup>1,\*</sup>, Jun-Long Zhao<sup>1,\*</sup>, Yan-Hui Zhou<sup>1</sup>, Biao-Liang Ye<sup>1</sup>, Yu-Liang Fang<sup>1</sup>, Yi-Hao Kang<sup>2</sup>, Qi-Ping Su<sup>2</sup>, Zheng-Wei Zhou<sup>3,4,5,†</sup>, and Chui-Ping Yang<sup>2,‡</sup>

<sup>1</sup>Quantum Information Research Center and Jiangxi Province Key Laboratory of Applied Optical Technology, Shangrao Normal University, Shangrao 334001, China

<sup>2</sup>School of Physics, Hangzhou Normal University, Hangzhou

<sup>3</sup>CAS Key Lab of Quantum Information, University of Science and Technology of China, Hefei 230026, China

<sup>4</sup>Anhui Center for fundamental sciences in theoretical physics,

University of Science and Technology of China, Hefei 230026, China

<sup>5</sup>Hefei National Laboratory, University of Science and Technology of China, Hefei 230088, China Zhejiang 311121, China

Nontrivial spectral properties of non-Hermitian systems can give rise to intriguing effects that lack counterparts in Hermitian systems. For instance, when dynamically varying system parameters along a path enclosing an exceptional point (EP), chiral mode conversion occurs. A recent study [Phys. Rev. Lett. 133, 113802 (2024)] demonstrates the achievability of pure adiabatic state transfer by specifically selecting a trajectory in the system parameter space where the corresponding evolution operator exhibits a real spectrum while winding around an EP. However, the intended adiabatic state transfer becomes fragile when taking into account the effect of the nonadiabatic transition. In this work, we propose a scheme for achieving robust and rapid adiabatic state transfer in time-modulated two-level non-Hermitian systems by appropriately modulating the system Hamiltonian and time-evolution trajectory. Numerical simulations confirm that a complete adiabatic transfer can always be achieved even under nonadiabatic conditions after one period for different initialized adiabatic states, and the scheme remains insensitive to moderate fluctuations in control parameters. Therefore, this scheme offers alternative approaches for quantum-state engineering in non-Hermitian systems.

PACS numbers: 03.67. Pp, 03.67. Mn, 03.67. HK

Keywords: Shortcuts to adiabaticity; Adiabatic state transfer; Non-Hermitian Hamiltonian; Exceptional points

## I. INTRODUCTION

In recent decades, there has been a growing interest in physical systems described by non-Hermitian (NH) Hamiltonians due to their unique spectral properties [1–3]. These systems can exhibit points of extreme degeneracy in the spectrum, known as exceptional points (EPs), where both eigenvalues and corresponding eigenmodes coalesce [4–8]. Structures supporting EPs have inspired numerous counterintuitive phenomena such as extreme sensitivity to perturbations [9], loss-induced transparency effects [10, 11], special topological structures [12, 13], and so on.

Recently studies have also revealed that the variation of system parameters along a path encircling EPs can induce chiral mode switching [13–24]. For instance, based on hopping, Li et al. demonstrated a robust switching of chiral modes in coupled waveguides on a standard silicon-on-insulator platform [16]. Additionally, Feilhauer et al. theoretically and experimentally demonstrated that a chiral state transfer can be achieved by manipulation of a dissipative Hamiltonian encircling an exceptional point

(EP) [17]. Arkhipov et al. further showcased the recovery of state flip symmetry in dissipative systems by applying nonadiabatic transformations in multimode systems and exploiting the spectral topology of hybrid diabolic-exceptional points [18]. Moreover, several studies have indicated that dynamical flip-state asymmetry can occur even when dynamically approaching EPs without necessarily encircling them [21, 22, 24]. Hassan et al. provided evidence that a sufficiently slow variation of parameters away from an exceptional point can still result in robust asymmetric state exchange [21]. More recently, in contrast to chiral or asymmetric mode conversion schemes, Arkhipov et al. achieved symmetric state transfer by intentionally selecting a trajectory in the system parameter space where the corresponding evolution operator acquires a real spectrum [25]. The aforementioned conventional encircling schemes offer promising pathways for manipulating quantum states in NH domains. However, a common challenge encountered with these schemes is the difficulty in achieving perfect adiabatic evolution in certain experiments, where the slow nature of adiabatic evolution may lead to decoherence effects due to interactions between the quantum system and its environment [26–28]. Therefore, it is crucial to explore innovative approaches that demonstrate both robustness and efficiency, serving as viable alternatives or enhancements to conventional encircling techniques.

The previously-reported generalized approximate adi-

\*These authors contributed equally to this work.

†E-mail: zwzhou@ustc.edu.cn

‡E-mail: yangcp@hznu.edu.cn

adiabaticity criterion in the NH system can be expressed as [29–33]

$$\sum_{n \neq m} \frac{|\langle \widehat{\phi}_n(t) | \dot{\phi}_m(t) \rangle|}{|\omega_{nm}(t)|} e^{i \int_0^t \omega_{nm}(\tau) d\tau} \ll 1, \quad (1)$$

where  $\{\widehat{\phi}_n(t)\}$  and  $\{\phi_m(t)\}$  are left and right eigenstates of the NH Hamiltonian  $H(t)$ ,  $\omega_{nm}(t) = E_m(t) - E_n(t)$  is the difference between corresponding eigenvalues of the NH Hamiltonian, and  $\langle \widehat{\phi}_n(t) | \dot{\phi}_m(t) \rangle$  is associated with the so-called nonadiabatic coupling transition between the instantaneous eigenstates. It is worth noting that in NH systems, the eigenvalues are typically complex values. The exponential function of the difference in imaginary parts of the eigenvalues ( $\exp[-\text{Im}[\omega_{nm}(t)]]$ ) can lead to either damping or amplification of the evolving state. Moreover, even a trivial difference between two eigenvalues can result in nontrivial changes in system dynamics if the trajectory of adiabatic evolution crosses EPs. Generally, nonadiabatic couplings become more pronounced as the speed of system evolution increases without external control. Interestingly, these nonadiabatic couplings can be nullified by applying so-called shortcuts to adiabaticity (STA) [34–36]. The critical idea behind STA is to accelerate quantum system dynamics through a designed coherent control, such that the system evolves on timescales much shorter than decoherence times. Based on this innovative concept, several methods have been proposed [37–45], including counter-diabatic driving (equivalently known as transitionless quantum algorithm) [37–40], Lewis-Riesenfeld inverse engineering [41–43], and "fast-forward" scaling techniques [44, 45], and so on.

Motivated by the remarkable advancements in state transfer within non-Hermitian systems through dynamic encircling of exceptional points [13–24] and shortcuts to adiabaticity [29–33], we aim to address the following question: Can perfect shortcuts to adiabatic state transfer be achieved in time-modulated non-Hermitian systems? The answer is affirmative. In this work, we demonstrate how a modified time-modulated non-Hermitian system can be used to realize shortcuts to adiabatic state transfer by encircling approximate EPs. Specifically, the adiabatic states correspond to eigenstates of a time-modulated two-level non-Hermitian Hamiltonian  $H_0$  with EPs, while the designed modified time-modulated non-Hermitian Hamiltonian  $H_m$  for shortcuts to adiabaticity does not possess any exact EP but exhibits an approximate EP where the eigenenergy spectrum is minimally separated. By designing a trajectory for the modified system's time evolution that closely approaches this approximate EP, robust and rapid adiabatic state transfer can be faithfully achieved. Different from conventional encircling schemes [13–25] which work under the adiabatic approximation condition, our scheme could nullify potential nonadiabatic coupling by applying some designed coherent controls, then it works well under the nonadiabatic approximation condition. A complete adiabatic

transfer can always be obtained after one period for different parameters and initialized states, and the initial adiabatic state can eventually return to itself after two periods. Moreover, the scheme demonstrates a good control performance and robustness in view of fluctuations of control parameters.

The rest sections of this paper are organized as follows. In Section II, we provide a concise overview of a symmetric state transfer scheme in a two-level NH Hamiltonian system, accompanied by an in-depth analysis of the effects of non-adiabatic transitions. Section III is dedicated to explicit discussions on how to engineer the NH Hamiltonian for constructing shortcuts to adiabatic state transfer and designing appropriate trajectories for system time evolution away from approximate exceptional points (EPs). The feasibility and performance of shortcuts to adiabatic state transfer are comprehensively discussed step by step. Finally, we present a summary in Section IV.

## II. CONVENTIONAL ADIABATIC STATE TRANSFER

Consider a two-level NH Hamiltonian [25]

$$H_0 = (k + i\kappa)\sigma_x + (\varepsilon - i\Delta)\sigma_z, \quad (2)$$

where  $\sigma_x$  and  $\sigma_z$  are Pauli matrices, and  $k, \kappa, \varepsilon, \Delta \in \mathbf{R}$ . A possible realization of such a system is two coupled dissipative cavities (in the mode representation) [25, 46–48], where  $\Delta$  ( $-\Delta$ ) denotes the resonator gain (loss) rate and  $\varepsilon$  is the frequency detuning of the resonators. The resonators are coupled coherently with interaction strength  $k$ , while  $\kappa$  accounts for dissipative coupling strength.

The eigenvalues of the NH Hamiltonian

$$\begin{aligned} E_{\pm} &= \pm \sqrt{E_1 E_2}, \\ E_1 &= k(t) - \Delta - i(\varepsilon - \kappa), \\ E_2 &= k(t) + \Delta + i(\varepsilon + \kappa), \end{aligned} \quad (3)$$

are complex, and one can not intuitively obtain much information about them except EPs  $\{\Delta_{EP}=k, \varepsilon_{EP}=\kappa\}$  and  $\{\Delta_{EP}=-k, \varepsilon_{EP}=-\kappa\}$ . However, with the help of a certain function  $f : \vec{r} = (x, y) \rightarrow (k, \kappa, \varepsilon, \Delta)$  as follows [25, 49, 50]:

$$\begin{aligned} k &= \alpha \cosh \phi_i \sin \phi_r, \quad \kappa = \alpha \sinh \phi_i \cos \phi_r, \\ \varepsilon &= \alpha \cosh \phi_i \cos \phi_r, \quad \Delta = \alpha \sinh \phi_i \sin \phi_r, \end{aligned} \quad (4)$$

where  $\phi = \phi_r + i\phi_i = \arctan[(x + iy)^{-1}] \in \mathbf{C}$ ,  $\alpha = x \sinh \phi_i / \sin \phi_r \in \mathbf{R}$ , the NH Hamiltonian in Eq. (2) acquires a simplified form

$$H_0 = \alpha(t) \begin{pmatrix} \cos \phi & \sin \phi \\ \sin \phi & -\cos \phi \end{pmatrix}. \quad (5)$$

It is not hard to find that  $H_0$  has real eigenvalues  $E_{\mp} = \mp \alpha$  and the corresponding right eigenvectors are

$$|\phi_{-}\rangle = [-\sin \frac{\phi}{2}, \cos \frac{\phi}{2}]^T,$$

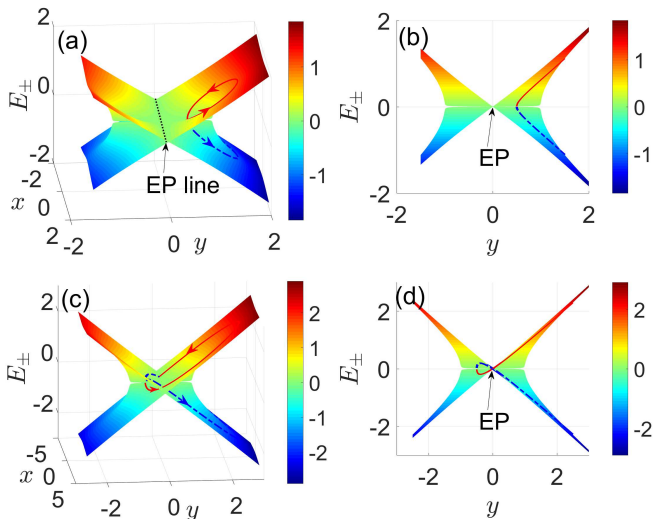


FIG. 1: The eigenenergy spectrum  $E_{\pm}(x, y)$  and the system's time-evolution trajectory  $E_{\pm}(x(t), y(t))$  of the non-Hermitian Hamiltonian  $H_0(t)$  given in Eq. (5) are depicted. The two energy Riemann surfaces (the red surface corresponds to  $E_{-}(x, y)$  and the blue surface corresponds to  $E_{+}(x, y)$ ) are connected by a line of exceptional points at  $y = 0$ . The solid red line represents  $E_{-}(t)$ , while the dashed blue line denotes  $E_{+}(t)$ . In panels (a) and (b) [(c) and (d)], identical parameters ( $r = 0.5, \omega = \pi/100, \phi_0 = \pi$ ) [ $r = 1.5, \omega = \pi/100, \phi_0 = \pi$ ] are used. The eigenenergy spectrum is presented as a three-dimensional surface in panels (a) and (c), whereas it is shown as a two-dimensional plot in panels (b) and (d).

$$|\phi_{+}\rangle = [\cos \frac{\phi}{2}, \sin \frac{\phi}{2}]^T, \quad (6)$$

where  $T$  stands for transpose. Together with the left eigenvectors

$$\begin{aligned} |\widehat{\phi}_{-}\rangle &= [-\sin \frac{\phi}{2}, \cos \frac{\phi}{2}]^T, \\ |\widehat{\phi}_{+}\rangle &= [\cos \frac{\phi}{2}, \sin \frac{\phi}{2}]^T, \end{aligned} \quad (7)$$

where the asterisk means complex conjugate. The biorthogonal partners  $\{|\widehat{\phi}_n\rangle\}$  and  $\{|\phi_m\rangle\}$  ( $n, m = +, -$ ) are normalized to satisfy the biorthogonality relation [3, 51]

$$\langle \widehat{\phi}_n | \phi_m \rangle = \delta_{nm}, \quad (8)$$

and the closure relation

$$\sum_n |\widehat{\phi}_n\rangle \langle \phi_n| = \sum_n |\phi_n\rangle \langle \widehat{\phi}_n| = 1. \quad (9)$$

### A. System eigenenergy spectrum and time-evolution trajectory

To gain an intuitive understanding of the energy change in the system, we present the eigenenergy spectrum  $E_{\pm}$  in the parameter space  $(x, y)$  using both

three-dimensional plots [Figs. 1(a) and (c)] and two-dimensional plots [Figs. 1(b) and (d)]. As depicted in Figs. 1(a) and (c), two energy Riemann surfaces are connected by an exceptional line  $y = 0$ , where all exceptional points reside. Mathematically, the phase parameter  $\phi = \phi_r + i\phi_i = \arctan[1/x]$  is a real parameter when setting  $y = 0$ . Consequently, it follows that  $\sinh \phi_i = 0$  and  $\alpha = x \sinh \phi_i / \sin \phi_r = 0$ . This observation is remarkable as it implies that EPs exist extensively in the parameter space  $(x, y)$ , allowing for easy identification of appropriate system time-evolution trajectories that encircle or approach these EPs.

For instance, a system time-evolution trajectory can be chosen as [25]

$$x(t) = r \sin(\omega t + \phi_0), y(t) = 1 - r \cos(\omega t + \phi_0), \quad (10)$$

where  $r, \omega, \phi_0 \in \mathbf{R}$  are constants, and the time  $t$  is presented in arbitrary units. Based on Eq. (10), the NH Hamiltonian  $H_0(t)$  undergoes periodic changes with respect to time  $t$  (with a period of  $T=2\pi/\omega$ ). The time-evolution trajectories of  $E_{\pm}(t)$  are also depicted in Fig. 1, where the solid red line represents  $E_{-}(t)$  and the dashed blue line denotes  $E_{+}(t)$ . The initial phase  $\phi_0 = \pi$  corresponds to the maximum separation between the two energy levels,  $E_{\pm}(t)$ . It can be observed that both orbiting trajectories of  $E_{\pm}(t)$  form irregular circles around the EPs, undergoing slight shape variations near these points. For positive angular frequencies ( $\omega > 0$ ), the orbiting trajectory proceeds counterclockwise (or clockwise). Furthermore, we emphasize that the radius, denoted as  $r$ , plays a crucial role in this dynamic process. When  $r < 1$  [see Figs. 1 (a) and (b)], the loops of time-evolution trajectory for  $E_{\pm}(t)$  remain distant from the exceptional lines, moving solely within a fixed plane of energy spectrum. However, when  $r \geq 1$  [see Fig. 1 (c) and (d)], these loops cross over at  $(\pm\sqrt{r^2 - 1}, 0)$  onto an opposite plane of energy spectrum during  $\tau \in [\tau_1 | x(\tau_1) = -\sqrt{r^2 - 1}, \tau_2 | x(\tau_2) = \sqrt{r^2 - 1}]$ , before returning back to their original plane in energy spectrum. It is worth noting that there is only a small difference in eigenvalues  $\omega_{nm}(t)$  when approaching times close to  $\tau_1, \tau_2$ .

### B. Performance of adiabatic state transfer

Now we proceed to elaborate on the performance of the adiabatic state transfer while dynamically encircling an exceptional point. The fidelity for the right eigenstate  $|\phi_n(t)\rangle$  ( $n = +, -$ ) is determined by the relation  $F_n = |\langle \widehat{\phi}_n(t) | \Psi(t) \rangle|^2$ , where  $|\Psi(t)\rangle$  represents the evolving state of the system at time  $t$ . Assuming that the system is initially prepared in one of its right eigenstates, i.e.,  $|\Psi(t=0)\rangle = |\phi_{-}(t=0)\rangle$ , we can obtain the evolving state  $|\Psi(t)\rangle$  through numerical integration of Schrödinger's equation. The instantaneous left eigenvector  $\langle \widehat{\phi}_n(t) |$  can be calculated by substituting the parameters into Eqs. (7) and (10).

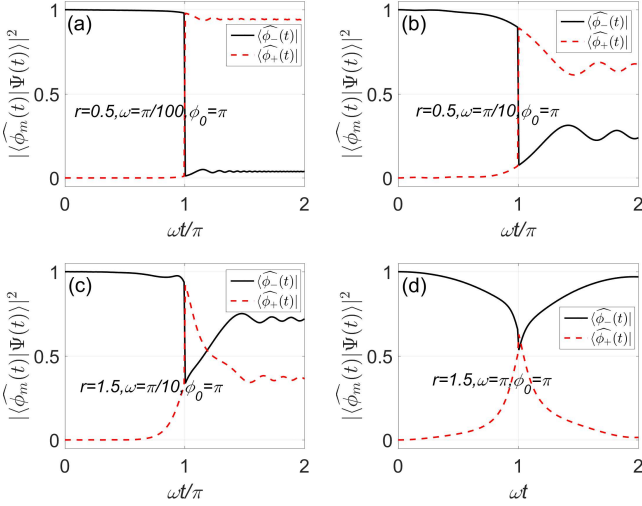


FIG. 2: The time evolution of fidelity  $F_n = |\langle \hat{\phi}_n(t) | \Psi(t) \rangle|^2$  for the time-dependent right eigenstate  $|\phi_n(t)\rangle$  ( $n=+, -$ ). The initial state is chosen as  $|\Psi(0)\rangle = |\phi_-(0)\rangle$  [see Eq. (6)] and other parameters are set as follows: (a)  $\{r = 0.5, \omega = \pi/100, \phi_0 = \pi\}$ , (b)  $\{r = 0.5, \omega = \pi/10, \phi_0 = \pi\}$ , (c)  $\{r = 1.5, \omega = \pi/10, \phi_0 = \pi\}$ , (d)  $\{r = 1.5, \omega = \pi, \phi_0 = \pi\}$ .

For the sake of convenience, in Fig. 2, we present the temporal evolution of the fidelity for eigenstate states with four sets of parameters: (a)  $\{r = 0.5, \omega = \pi/100, \phi_0 = \pi\}$ , (b)  $\{r = 0.5, \omega = \pi/10, \phi_0 = \pi\}$ , (c)  $\{r = 1.5, \omega = \pi/10, \phi_0 = \pi\}$ , (d)  $\{r = 1.5, \omega = \pi, \phi_0 = \pi\}$ . Figure 2(a) exhibits a relatively complete eigenstate transfer, where  $|\phi_-(t)\rangle \leftrightarrow |\phi_+(t)\rangle$  are exchanged after one period  $T=2\pi/\omega$ . However, it is regrettable that the final fidelity falls short for practical applications. Moreover, as depicted in Figs. 2(b)-(d), the state transfer fails entirely when there are dynamic variations in the parameters  $(x(t), y(t))$ , i.e., when  $\omega$  or  $r$  takes on large values. In fact, there are two potential physical mechanisms involved in the entire dynamic process: (i) under perfect adiabatic conditions, if the system's time-evolution trajectory winds around or approaches EPs, a perfect state transformation occurs within half a period, and the transferred state will be preserved due to the adiabatic effect. (ii) When the adiabatic conditions are not perfectly satisfied, nonadiabatic coupling transitions between instantaneous eigenstates always occur, leading to the destruction of desired state transfer throughout the evolutionary process. It is worth noting that the adiabatic conditions [see Eq. (1)] is also associated with the difference in eigenvalues  $\omega_{nm}(t)$  of the system. If the system's time-evolution trajectory passes through EPs  $(x(t) = \pm\sqrt{r^2-1}, y(t) = 0)$ , as shown in Fig. 1 (c) and (d), temporarily amplified effects of nonadiabatic coupling transitions may arise.

The aforementioned mechanisms can be employed to comprehend the phenomena depicted in Fig. 2. In Fig. 2(a), under a suitable adiabatic condition, mechanism (i) predominantly governs the system evolution,

while the adverse impact of mechanism (ii) leads to fidelity fluctuations throughout the process. Furthermore, upon comparing Fig. 2(a) with Fig. 2(b), it becomes evident that the adiabatic conditions in Fig. 2(b) are worse due to a large  $\omega$ , thereby amplifying the role of mechanism (ii) during the system evolution and causing rapid fidelity degradation. Moreover, in Fig. 2(c), when  $r=1.5>1$ , it implies that the time-evolution trajectory crosses the exceptional line at  $(\pm\sqrt{r^2-1}, 0)$ , triggering two instances of significant added-state transformations through enhanced manifestation of mechanism (ii). Consequently, compared to results obtained from Fig. 2(b), significant state transitions occur precisely when  $\tau_1|x(\tau_1) = -\sqrt{r^2-1}$  and  $\tau_2|x(\tau_{21}) = \sqrt{r^2-1}$ . Finally, in Fig. 2(d), due to an extremely poor performance of adiabatic conditions, mechanism (ii) overwhelmingly dominates the system evolution. Therefore, achieving flawless state transition necessitates minimizing the nonadiabatic coupling transition effects as much as possible and avoiding the trajectory passage through exceptional points during the system evolution.

### III. SHORTCUTS TO ADIABATIC STATE TRANSFER

It is advisable to project the system into the so-called adiabatic frame  $\{|\phi_+(t)\rangle, |\phi_-(t)\rangle\}$ , with  $H_0^a(t) = \tilde{R}^\dagger(t)H_0(t)R(t) - i\hbar\tilde{R}^\dagger(t)\dot{R}(t)$ , where the transformation matrixes  $R(t)$  and  $\tilde{R}^\dagger(t)$  are given by

$$R(t) = \begin{pmatrix} \cos \frac{\phi(t)}{2} & -\sin \frac{\phi(t)}{2} \\ \sin \frac{\phi(t)}{2} & \cos \frac{\phi(t)}{2} \end{pmatrix},$$

$$\tilde{R}^\dagger(t) = \begin{pmatrix} \cos \frac{\phi(t)}{2} & \sin \frac{\phi(t)}{2} \\ -\sin \frac{\phi(t)}{2} & \cos \frac{\phi(t)}{2} \end{pmatrix}. \quad (11)$$

Then, the original Hamiltonian  $H_0(t)$  in the adiabatic basis can be written as

$$H_0^a(t) = \begin{pmatrix} E_+(t) & 0 \\ 0 & E_-(t) \end{pmatrix} - i\hbar \begin{pmatrix} 0 & -\dot{\phi}(t)/2 \\ \dot{\phi}(t)/2 & 0 \end{pmatrix}, \quad (12)$$

where

$$\dot{\phi}(t) = -\frac{[\dot{x}(t)a(t) + \dot{y}(t)b(t) + i(\dot{y}(t)a(t) - \dot{x}(t)b(t))]}{a^2(t) + b^2(t)},$$

$$a(t) = 1 + x^2(t) + y^2(t), \quad b(t) = 2x(t)y(t). \quad (13)$$

The adiabatic process can be regarded as a two-level toy model driven simultaneously by a coherent field  $\Omega_0(t)$  and an incoherent field  $\Omega_1(t)$ . It is evident that under the conditions

$$|\Omega_0(t)|, |\Omega_1(t)| \ll E_+ - E_-, \quad (14)$$

with  $\Omega_0(t) = \text{Re}[\dot{\phi}(t)/2]$  and  $\Omega_1(t) = \text{Im}[\dot{\phi}(t)/2]$ , the transitions between the adiabatic states will be significantly suppressed due to rapid oscillations. However, in the

event that the condition fails to meet the required criteria, nonadiabatic coupling transitions may emerge as the predominant factor influencing the system evolution.

### A. Modified effective Hamiltonian and time-evolution trajectory

The STA theory (transitionless quantum driving [34–40]) provides an effective approach to achieve the state transfer without relying on the adiabatic condition through modifications to the system's Hamiltonian. Moreover, the modified effective Hamiltonian can be calculated by

$$H_m(t) = H_0(t) + H_1(t), \quad (15)$$

where

$$\begin{aligned} H_1(t) &= i\hbar\tilde{R}^\dagger(t)\dot{R}(t) \\ &= i\hbar\begin{pmatrix} 0 & -\frac{\dot{\phi}(t)}{2} \\ \frac{\dot{\phi}(t)}{2} & 0 \end{pmatrix}. \end{aligned} \quad (16)$$

Theoretically, the system is driven along adiabatic paths defined by  $H_0(t)$  through  $H_m(t)$ . However, implementing the added term  $H_1(t)=\dot{\phi}(t)/2\sigma_y$  in practice is not straightforward. Specifically,  $\dot{\phi}(t)$  is often a complex number, resulting in non-complex conjugate off-diagonal terms. Therefore, it is advisable to set  $\dot{\phi}(t)=\text{Re}[\dot{\phi}(t)]$ , which offers two distinct advantages: (i) the practical realization of  $H_1(t)$  becomes easier (here  $H_1(t)$  can be considered as a coherent field  $\Omega_0(t)$  with a fixed phase  $e^{\frac{\pi}{2}}$ ); (ii) the eigenvalues of the modified effective Hamiltonian  $H_m(t)$  remain real values  $E'_\pm=\pm\sqrt{\text{Re}[\dot{\phi}(t)]^2/4+\alpha^2(t)}$  across all parameter ranges  $(x(t), y(t))$ .

The elimination of  $\text{Im}[\dot{\phi}(t)]$  can be achieved by satisfying the following equation

$$-\dot{x}(t)b(t) = \dot{y}(t)a(t), \quad (17)$$

with  $a(t)=1+x^2(t)+y^2(t)$ ,  $b(t)=2x(t)y(t)$ . After performing algebraic calculations, we derive a modified trajectory for the time evolution of the system

$$\begin{aligned} x(t) &= r \sin(\omega t + \phi_0), \\ y'(t) &= \sqrt{1+r^2-r} \cos(\omega t + \phi_0). \end{aligned} \quad (18)$$

We emphasize that the modified trajectory for the time-evolution of the system cloud ensure the elimination of  $\text{Im}[\dot{\phi}(t)]$  and prevents the system time-evolution trajectory from crossing the exceptional line  $y=0$  of  $H_0(t)$  ( $y'(t)\neq 0$ ). It should be noted that the choice of the trajectory in Eq. (18) is not unique, allowing for flexibility based on different situations.

Up to now, we have successfully accomplished the design of shortcuts to adiabatic state transfer and system time-evolution trajectory, yielding the subsequent modified NH Hamiltonian

$$H_m(t) = [k(t) + i\kappa(t)]\sigma_x + \Omega(t)\sigma_y + [\varepsilon(t) - i\Delta(t)]\sigma_z \quad (19)$$

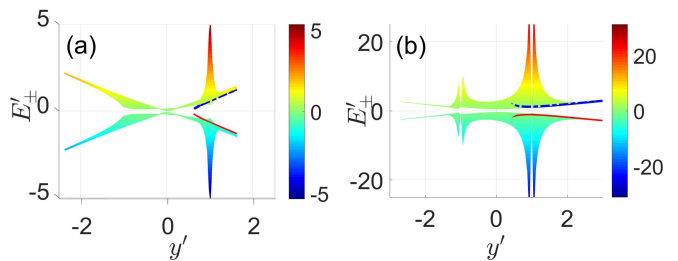


FIG. 3: The eigenenergy spectrum  $E'_\pm(x, y')$  and the system's time-evolution trajectory  $E'_\pm(x(t), y'(t))$  of the NH Hamiltonian  $H_0(t)$  given in Eq. (5) are presented. Two energy surfaces, with the blue surface corresponding to  $E'_-(x, y)$  and the red surface corresponding to  $E'_+(x, y)$ , are clearly separated. The solid red line represents  $E'_-(t)$  while the dashed blue line denotes  $E'_+(t)$ . In (a) and (b), we consider parameters ( $r = 0.5, \omega = \pi/10, \phi_0 = \pi$ ) and ( $r = 1.5, \omega = \pi/10, \phi_0 = \pi$ ), respectively.

where

$$\begin{aligned} k(t) &= \alpha(t) \cosh \phi_i(t) \sin \phi_r(t), \\ \kappa(t) &= \alpha(t) \sinh \phi_i(t) \cos \phi_r(t), \\ \varepsilon(t) &= \alpha(t) \cosh \phi_i(t) \cos \phi_r(t), \\ \Delta(t) &= \alpha(t) \sinh \phi_i(t) \sin \phi_r(t), \\ \Omega(t) &= \dot{\phi}(t)/2, \end{aligned} \quad (20)$$

with  $\phi(t)=\phi_r(t)+i\phi_i(t)=\arctan[(x(t)+iy'(t))^{-1}] \in \mathbf{C}$ ,  $\alpha(t)=x(t) \sinh \phi_i(t) / \sin \phi_r(t)$ ,  $\dot{\phi}(t) \in \mathbf{R}$ . From an experimental perspective, the modified NH Hamiltonian can be derived in the two-mode approximation for countertraveling waves in a whispering-gallery microcavity, such as a micro-disk or micro-toroid, perturbed by  $N$  Rayleigh scatterers [46–48]. The effective Hamiltonian in the traveling-wave basis (counterclockwise (CCW), clockwise (CW)) is.

$$H^{(M)} = \begin{pmatrix} \omega^{(M)} & A^{(M)} \\ B^{(M)} & \omega^{(M)} \end{pmatrix}, \quad (21)$$

where  $\omega^{(M)}=\omega_0+\sum_{j=1}^M \varepsilon_j$ ,  $A^{(M)}=\sum_{j=1}^M \varepsilon_j e^{-i2k\beta_j}$  and  $B^{(M)}=\sum_{j=1}^M \varepsilon_j e^{i2k\beta_j}$ . Here,  $m$  is the azimuthal mode number,  $\omega_0$  is the complex frequency of the unperturbed resonance mode,  $\beta_j$  is the angular position of scatterer  $j$ , and  $\varepsilon_j$  is the complex frequency splitting that is introduced by scatterer  $j$  alone. Notably, due to the asymmetry in backscattering between clockwise- and anticlockwise-travelling waves, it is possible for  $|A^{(M)}|$  to differ from  $|B^{(M)}|$ .

### B. Performance of shortcuts to adiabatic state transfer

Before elaborating on the performance of the scheme for a complete fidelity transfer, we also briefly evaluate the eigenenergy spectrum of  $H_m(t)$ . We plot the

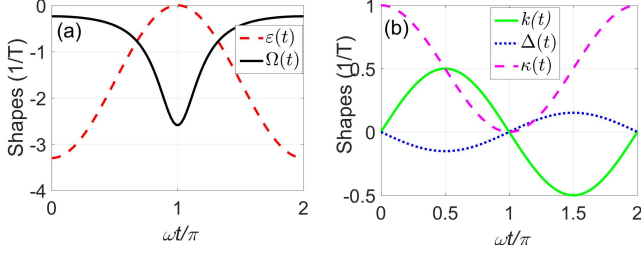


FIG. 4: The shapes of the time-modulated system parameters in Eq. (20) are depicted when winding counterclockwise in the chart  $(x, y')$ , as described by Eq. (18). (a) The frequency detuning  $\varepsilon(t)$  is represented by a red dashed curve, while the coupling strength  $\Omega(t)$  is shown as a black solid curve. (b) The coherent mode coupling strength  $k(t)$  is illustrated with a green solid curve, and the gain-loss rate  $\Delta(t)$  is displayed using a blue dot dash curve. Additionally, the incoherent mode coupling strength  $\kappa(t)$  is presented as a pink dashed curve. The parameters have been set to  $r = 1.5, \omega = \pi/10, \phi_0 = \pi$ .

eigenenergy spectrum  $E'_\pm = \pm \sqrt{\Omega^2(t) + \alpha^2(t)}$  in the parameter space  $(x, y')$ . As shown in Figs. 3(a) and (b), two energy surfaces (the red surface belonging to  $E_+$  and blue surface belonging to  $E_-$ ) are separated. This indicates that there are no EPs in the modified NH Hamiltonian. Although  $y'=0$  is no longer an EP line, the two eigenenergy spectra  $E_\pm(x, y')$  remain minimally separated near it, which can be considered as an approximate EP (AEP) line. Importantly, regardless of arbitrary choices for radius  $r$  and frequency  $\omega$ , the system's time-evolution trajectory will not cross this AEP line. This result has immediate implications for potentially reducing experimental implementation difficulties associated with certain parameters. The shapes of the time-modulated system parameters in Eq. (19) are plotted in Fig. 4, illustrating their counterclockwise winding direction in chart  $(x, y')$  according to Eq. (18) with parameters  $r = 1.5, \omega = \pi/10, \phi_0 = \pi$ . The shapes of the time-modulated system parameters can be readily observed using current experimental techniques [46–48], as they exhibit a remarkable simplicity.

In Fig. 5, we present the temporal evolution of the fidelity for the adiabatic states with two sets of parameters ( $r = 0.5, \omega = \pi/10, \phi_0 = \pi$ ) and ( $r = 1.5, \omega = \pi, \phi_0 = \pi$ ) under different initial states. It is evident that, in contrast to the conventional adiabatic state transfer case (see Fig. 2), which fails when either  $\omega$  or  $r$  takes large values, a complete adiabatic transfer, i.e.,  $|\phi_-(t)\rangle \leftrightarrow |\phi_+(t)\rangle$ , can always be achieved after one period  $T = 2\pi/\omega$ , regardless of the initialized adiabatic states and control parameters employed, thus validating our theoretical deduction. Furthermore, it is noteworthy that the initial state eventually returns to itself after two periods ( $2T = 4\pi/\omega$ ).

In the preceding discussion, the potential impact of parameter fluctuations has not been thoroughly examined. Therefore, it is imperative to investigate the sensitivity of the shortcuts to adiabatic state transfer in relation

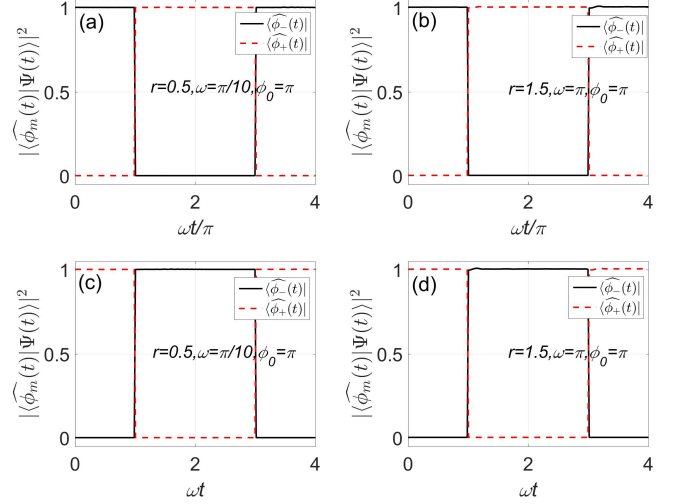


FIG. 5: The time evolution of the fidelity  $F_n = |\langle \widehat{\phi}_n(t) | \Psi(t) \rangle|^2$  for the time-dependent right eigenstate  $|\phi_n(t)\rangle$  ( $n = +, -$ ). The initialized state in (a) and (b) [ $|\Psi(0)\rangle = |\phi_-(0)\rangle$ ] [ $|\Psi(0)\rangle = |\phi_+(0)\rangle$ ], the parameters in (a) and (c) [(b) and (d)] are chosen as  $\{r = 0.5, \omega = \pi/10, \phi_0 = \pi\}$  [ $\{r = 1.5, \omega = \pi, \phi_0 = \pi\}$ ], respectively.

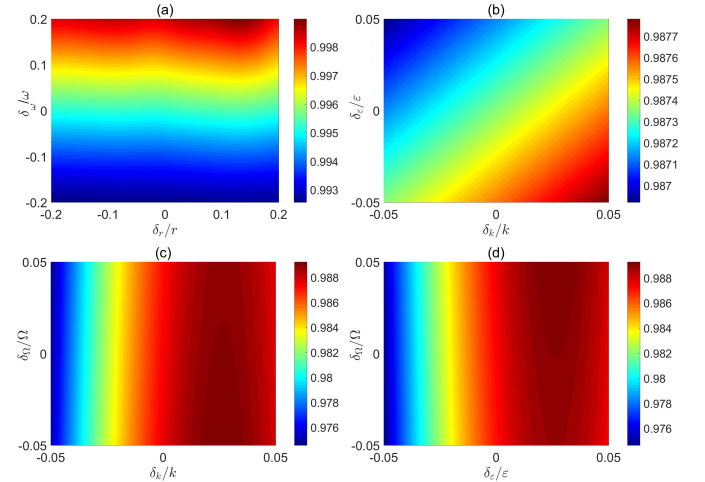


FIG. 6: The fidelity of  $F_+ = |\langle \widehat{\phi}_+(T) | \Psi(T) \rangle|^2$  vs several relative deviations in the control parameters. (a)  $\delta_r/r, \delta_\omega/\omega$ , (b)  $\delta_k/k, \delta_\varepsilon/\varepsilon$ , (c)  $\delta_k/k, \delta_\Omega/\Omega$ , (d)  $\delta_\varepsilon/\varepsilon, \delta_\Omega/\Omega$ . The other parameters are chosen as  $r = 1.5, \omega = 100\pi, \phi_0 = \pi$ .

to simulated variations in control parameters. Initially, we focus on analyzing the fluctuations in trajectory parameters  $\delta_r/r$  and  $\delta_\omega/\omega$ . Figure 6(a) demonstrates that the fidelity  $F_+ = |\langle \widehat{\phi}_+(T) | \Psi(T) \rangle|^2$  remains largely unaffected by these trajectory parameter fluctuations, with only minor variations at an order of magnitude around  $10^{-3}$ . This observation suggests that our designed system time-evolution trajectory is highly efficient and guarantees a complete eigenstate transfer even when there exists a range for trajectory parameters. Furthermore, we also consider fluctuations in control parameters as described

by Eq. (19). The results depicted in Figs. 6(a)-(c) reveal that a high fidelity (above 0.984) can be achieved within a broad range of control parameters indicated by the red area. Consequently, this scheme exhibits remarkable efficiency while relaxing constraints on control parameters.

#### IV. CONCLUSION

We have proposed a scheme to achieve robustness and fast adiabatic state transfer in time-modulated two-level non-Hermitian systems, by appropriately designing the system Hamiltonian and time-evolution trajectory, and considering the effects of non-adiabatic transitions. This approach contrasts with conventional encircling schemes, where the complex system spectrum, rapid winding speed, and vanishing eigenvalue differences (at exceptional points) often lead to significant nontrivial non-adiabatic transitions during the state evolution. Inspired by Ref. [25], we have transformed the NH Hamiltonian into a pseudo-Hermitian one with a real spectrum by suitably mapping the system parameter space onto a four-dimensional hyperboloid manifold. We have showed that potential nonadiabatic couplings under fast winding speeds can be nullified through a designed coherent control based on STA. Furthermore, we have designed the

system's time-evolution trajectory to avoid crossing exceptional points. Remarkably, these procedures enable complete adiabatic state transfers even in nonadiabatic scenarios after just one period for different initialized adiabatic states. The effects of variations in control parameters have been also extensively discussed. Our results demonstrate that this scheme exhibits insensitivity to moderate fluctuations of control parameters and one can obtain high fidelity over a wide range of parameter values. Therefore, the scheme is powerful and reliable for quantum-state engineering in non-Hermitian systems.

#### ACKNOWLEDGEMENT

This work was supported by National Natural Science Foundation of China (NSFC) (Grants Nos. 12264040, 12374333, 12474366, 12204311 and U21A20436), Jiangxi Natural Science Foundation (Grant Nos. 20232BCJ23022, 20224BAB201027, 20224BAB211025 and 20212BAB211018), Innovation Program for Quantum Science and Technology (Grant No. 2021ZD0301200) and the Jiangxi Province Key Laboratory of Applied Optical Technology (Grant No. 2024SSY03051).

- 
- [1] T. Kato, *Perturbation Theory for Linear Operators*, Classics in Mathematics (Springer, Berlin, 1995).
- [2] Y. Ashida, Z. Gong, and M. Ueda, Non-Hermitian physics, *Adv. Phys.* **69**, 249 (2020).
- [3] Q. C. Wu, J. L. Zhao, Y. L. Fang, Y. Zhang, D. X. Chen, C. P. Yang and F. Nori, Extension of Noether's theorem in PT-symmetry systems and its experimental demonstration in an optical setup, *Sci. China-Phys. Mech. Astron.* **66**(4), 240312 (2023).
- [4] L. Feng, R. El-Ganainy and L. Ge, Non-Hermitian photonics based on parity-time symmetry, *Nat. Photon.* **11**, 752 (2017).
- [5] Ş. Özdemir, S. Rotter, F. Nori, and L. Yang, Parity-time symmetry and exceptional points in photonics, *Nat. Mater.* **18**, 783 (2019).
- [6] W. D. Heiss, Repulsion of resonance states and exceptional points, *Phys. Rev. E* **61**, 929 (2000).
- [7] H. Cartarius, J. Main, and G. Wunner, Exceptional points in atomic spectra, *Phys. Rev. Lett.* **99**, 173003 (2007).
- [8] O. Atabek, R. Lefebvre, M. Lepers, A. Jaouadi, O. Dulieu, and V. Kokoouline, Proposal for a laser control of vibrational cooling in Na<sub>2</sub> using resonance coalescence, *Phys. Rev. Lett.* **106**, 173002 (2011).
- [9] H. Hodaei, A. U. Hassan, S. Wittek, H. Garcia-Gracia, R. El-Ganainy, D. N. Christodoulides, and M. Khajavikhan, Enhanced sensitivity at higher-order exceptional points, *Nature* **548**, 187 (2017).
- [10] Z. Lin, H. Ramezani, T. Eichelkraut, T. Kottos, H. Cao, and D. N. Christodoulides, Unidirectional invisibility induced by PT-symmetric periodic structures, *Phys. Rev. Lett.* **106**, 213901 (2011).
- [11] A. Guo, G. J. Salamo, D. Duchesne, R. Morandotti, M. Volatier-Ravat, V. Aimez, G. A. Siviloglou, and D. N. Christodoulides, Observation of PT-symmetry breaking in complex optical potentials, *Phys. Rev. Lett.* **103**, 093902 (2009).
- [12] E. J. Bergholtz, J. C. Budich, and F. K. Kunst, Exceptional topology of non-Hermitian systems, *Rev. Mod. Phys.* **93**, 015005 (2021).
- [13] C. Guria, Q. Zhong, Ş. K. Özdemir, Y. S. S. Patil, R. El-Ganainy, and J. G. Emmet Harris, Resolving the topology of encircling multiple exceptional points, *Nat. Commun.* **15**, 1369 (2024).
- [14] M. V. Berry, Optical polarization evolution near a non-Hermitian degeneracy, *J. Opt. A* **13**, 115701 (2011).
- [15] H. Xu, D. Mason, Luyao Jiang, and J. G. E. Harris, Topological energy transfer in an optomechanical system with exceptional points, *Nature (London)* **537**, 80 (2016).
- [16] A. Li, J. Dong, J. Wang, Z. Cheng, J. S. Ho, D. Zhang, et al., Hamiltonian hopping for efficient chiral mode switching in encircling exceptional points, *Phys. Rev. Lett.* **125**(18), 187403 (2020).
- [17] J. Feilhauer, A. Schumer, J. Doppler, A. A. Mailybaev, J. Böhm, U. Kuhl, N. Moiseyev, and S. Rotter, Encircling exceptional points as a non-Hermitian extension of rapid adiabatic passage, *Phys. Rev. A* **102**, 040201 (2020).
- [18] I. I. Arkhipov, A. Miranowicz, F. Minganti, Ş. Özdemir, and F. Nori, Dynamically crossing diabolic points while encircling exceptional curves: A programmable symmetric/asymmetric multimode switch, *Nat. Commun.* **14**, 2076 (2023).

- [19] M. S. Ergoktas, S. Soleymani, N. Kakenov, K. Wang, T. B. Smith, G. Bakan, S. Balci, A. Principi, K. S. Novoselov, S. K. Ozdemir, and C. Kocabas, Topological engineering of terahertz light using electrically tunable exceptional point singularities, *Science* **376**, 184 (2022).
- [20] Z. Tang, T. Chen, and X. Zhang, Highly efficient transfer of quantum state and robust generation of entanglement state around exceptional lines, *Laser Photonics Rev.* **2300794** (2023).
- [21] A. U. Hassan, G. L. Galmiche, G. Harari and P. LiKamWa, Chiral state conversion without encircling an exceptional point, *Phys. Rev. A* **96**, 052129 (2017).
- [22] A. U. Hassan, B. Zhen, M. Soljačić, M. Khajavikhan, and D. N. Christodoulides, Dynamically encircling exceptional points: Exact evolution and polarization state conversion, *Phys. Rev. Lett.* **118**, 093002 (2017).
- [23] X. L. Zhang, T. Jiang, and C. T. Chan, Dynamically encircling an exceptional point in anti-parity-time symmetric systems: Asymmetric mode switching for symmetrybroken modes, *Light Sci. Appl.* **8**, 88 (2019).
- [24] H. Nasari, G. L. Galmiche, H. E. L. Aviles, A. Schumer, A. U. Hassan, Q. Zhong, S. Rotter, P. LiKamWa, D. N. Christodoulides and M. Khajavikhan, Observation of chiral state transfer without encircling an exceptional point, *Nature* **605**, 256 (2022).
- [25] I. I. Arkhipov, A. Miranowicz, F. Minganti, Ş. Özdemir, and F. Nori, Restoring adiabatic state transfer in time-modulated non-hermitian systems, *Phys. Rev. Lett.* **133**, 113802, (2024)
- [26] F. Verstraete, M. M. Wolf and J. I. Cirac, Quantum computation and quantum-state engineering driven by dissipation, *Nat. Phys.* **5**(9), 633 (2009).
- [27] Q. C. Wu, Y. H. Zhou, B. L. Ye, T. Liu and C. P. Yang, Nonadiabatic quantum state engineering by time-dependent decoherence-free subspaces in open quantum systems, *New J. Phys.* **23**, 113005 (2021).
- [28] H. Zhang, X. K. Song, Q. Ai, H. Wang, G. J. Yang, and F. G. Deng, Fast and robust quantum control for multimode interactions using shortcuts to adiabaticity, *Opt. Express* **27**, 7384 (2019).
- [29] S. Ibáñez and J. G. Muga, Adiabaticity condition for non-Hermitian Hamiltonians, *Phys. Rev. A* **89**(3), 033403 (2014).
- [30] Q. C. Wu, Y. H. Chen, B. H. Huang, Y. Xia, and J. Song, Reverse engineering of a nonlossy adiabatic Hamiltonian for non-Hermitian systems, *Phys. Rev. A* **94**, 053421 (2016).
- [31] H. Li, H. Z. Shen, S. L. Wu, and X. X. Yi, Shortcuts to adiabaticity in non-Hermitian quantum systems without rotating-wave approximation, *Opt. Express* **25**, 30135 (2017).
- [32] Y. H. Chen, Q. C. Wu, B. H. Huang, J. Song, Y. Xia, and S. B. Zheng, Improving shortcuts to non-Hermitian adiabaticity for fast population transfer in open quantum systems, *Ann. Phys. (Berlin)* **530**, 1700247 (2017).
- [33] Luan, T. Z., H. Z. Shen, and X. X. Yi, Shortcuts to adiabaticity with general two-level non-Hermitian systems, *Phys. Rev. A*, **105**, 013714 (2022).
- [34] X. Chen, I. Lizuain, A. Ruschhaupt, D. Guéry-Odelin, and J. G. Muga, Shortcut to adiabatic passage in two and three-level atoms, *Phys. Rev. Lett.* **105**, 123003 (2010).
- [35] E. Torrontegui, S. Ibáñez, S. Martínez-Garaot, M. Modugno, A. del campo, D. Guéry-Odelin, A. Ruschhaupt, X. Chen, and J. G. Muga, Shortcuts to adiabaticity, *Adv. At. Mol. Opt. Phys.* **62**, 117 (2013).
- [36] D. Guéry-Odelin, A. Ruschhaupt, A. Kiely, E. Torrontegui, S. Martínez-Garaot and J. G. Muga, Shortcuts to adiabaticity: Concepts, methods, and applications, *Rev. Mod. Phys.* **91**(4) 045001 (2019).
- [37] M. Demirplak and S. A. Rice, Adiabatic population transfer with control fields, *J. Phys. Chem. A* **107**, 993715 (2003).
- [38] M. V. Berry, Transitionless quantum driving, *J. Phys. A* **42**(36), 365303 (2009).
- [39] G. Q. Li, G. D. Chen, P. Peng, and W. Qi, NonHermitian shortcut to adiabaticity of two-and threelevel systems with gain and loss, *Eur. Phys. J. D* **71**, 14 (2017).
- [40] Y. H. Chen, W. Qin, X. Wang, A. Miranowicz and F. Nori, Shortcuts to adiabaticity for the quantum rabi model: efficient generation of giant entangled cat states via parametric amplification, *Phys. Rev. Lett.* **126**(2) 023602 (2021).
- [41] H. R. Lewis and W. B. Riesenfeld, An exact quantum theory of the time-dependent harmonic oscillator and of a charged particle in a time-dependent electromagnetic field, *J. Math. Phys.* **10**, 1458 (1969).
- [42] X. Chen, E. Torrontegui and J. G. Muga, Lewis-Riesenfeld invariants and transitionless quantum driving, *Phys. Rev. A* **83**(6), n062116 (2011).
- [43] Y. H. Kang, Y. H. Chen, B. H. Huang, J. Song, and Y. Xia, Invariant-based pulse design for three-level systems without the rotating-wave approximation, *Ann. Phys. (Berlin)* **529**, 1700004 (2017).
- [44] S. Masuda and K. Nakamura, Fast-forward problem in quantum mechanics, *Phys. Rev. A* **78**, 062108 (2008).
- [45] J. J. Zhu and X. Chen, Fast-forward scaling of atom-molecule conversion in Bose-Einstein condensates, *Phys. Rev. A* **103**, 023307 (2021).
- [46] W. Chen, Ş. Özdemir, G. Zhao, J. Wiersig, and L. Yang, Exceptional points enhance sensing in an optical microcavity, *Nature (London)* **548**, 192 (2017).
- [47] I. I. Arkhipov, A. Miranowicz, F. Nori, Ş. K. Özdemir, and F. Minganti, Fully solvable finite simplex lattices with open boundaries in arbitrary dimensions, *Phys. Rev. Res.* **5**, 043092 (2023).
- [48] H. S. Xu and L. Jin, Coupling-induced nonunitary and unitary scattering in anti-PT-symmetric non-Hermitian systems, *Phys. Rev. A* **104**, 012218 (2021).
- [49] M. V. Berry, Physics of non-Hermitian degeneracies, *Czech. J. Phys.* **54**, 1039 (2004).
- [50] J. Maldacena, The large-N limit of superconformal field theories and supergravity, *Adv. Theor. Math. Phys.* **2**, 231 (1998).
- [51] D. C. Brody, Biorthogonal quantum mechanics, *J. Phys. A-Math. Theor.* **47**, 035305 (2013).